Ground Motion Simulation in an Urban Environment Considering Site-City Interaction: a Case Study of Kowloon Station, Hong K....

Conference Paper · August 2017

CITATIONS
0

READS
169

2 authors:

Bence Kato
The Hong Kong University of Science and Tec...
2 PUBLICATIONS **0** CITATIONS
SEE PROFILE

Gang Wang
The Hong Kong University of Science and Tec...
52 PUBLICATIONS **601** CITATIONS
SEE PROFILE

Ground Motion Simulation in an Urban Environment Considering Site-City Interaction: a Case Study of Kowloon Station, Hong Kong

B. Kato[1], G. Wang[2]

1 *PhD student, Dept. of Civil and Environmental Engineering, Hong Kong University of Science and Technology, Clear Water Bay, Kowloon, Hong Kong.*
E-mail: bkato@ust.hk

2 *Associate Professor, Dept. of Civil and Environmental Engineering, Hong Kong University of Science and Technology, Clear Water Bay, Kowloon, Hong Kong.*
E-mail: gwang@ust.hk

ABSTRACT
Seismic safety of congested metropolitan environments are of key importance for sustainable urban development. Closely spaced high-rise buildings are often adjacent to underground structures in settings such as transportation hubs that yield complex dynamic phenomena during earthquakes. Structures in megacities are nonetheless designed using conventional earthquake engineering practices despite reports on multiple interactions between soil and structures (SSSI), for instance erratic structural damage patterns after large earthquakes. This study is set to explore Soil-Underground structure-Soil Interaction (SUSSI) and Site-City Interaction (SCI) through realistic 3D models of Kowloon station, in Hong Kong. A discontinuous Galerkin spectral element method is adopted via the computational platform, SPEED that can efficiently deal with non-conforming meshes, thus easing some key challenges of complex 3D wave propagation problems. For comparative purposes two models are considered, one representing solely the building-foundation systems at the transportation hub, while the other includes a subsurface metro station. A viscoelastic layer-cake model represents the substratum; whereas the metro station and building-foundation systems are modelled by a closed rigid box and homogeneous block models capturing their principal dynamic and geometric properties, respectively. Key findings highlight SUSSI, SCI, moreover how special urban layouts, such as squares, along with structural weight distribution and foundation depth alter surface ground motions.

KEYWORDS: *3D Ground Motion Simulation, Site-City Interaction, SSSI, SUSSI, Urban Transportation Hub*

1. INTRODUCTION

Congested urban sites in municipalities represent the heart of the city in terms of population, socio-economical and transportation aspects alike. Hence, these sites necessitate cutting-edge engineering design and well-thought urban planning to guarantee both the safety of their structures and the comfort of their population. Despite their importance, the seismic design of such sites are carried out using conventional methods disregarding structure-soil-structure interaction (SSSI) and future expansions that can significantly change the demand on urban sites and their surroundings. Several pioneering works have reported the beating effect (Jennings, 1970) and communication between buildings through the soil (Gueguen & Bard., 2005). During earthquakes, buildings act as individual resonator sources sending feedback vibrations to the soil, which further interact with their surrounding structural environment. In support of these phenomena, erratic damage patterns and prolonged response of site and buildings have been observed in several instances, most notably in Mexico City after the 1985 earthquake (Flores, et al., 1987, Çelebi, et al., 2010). This rose the attention towards site-city interaction (SCI), as well as generated active effort towards understanding and describing the phenomenon (Guéguen, et al., 2002, Kham, et al., 2006, Semblat, et al., 2008, Taborda & Bielak., 2011, Schwan, et al., 2016). Although significant progress has been made on the topic of SSSI and SCI, fully integrated 3D analyses considering realistic above and underground settings of the cities are still lacking in the literature. However, several research groups have pointed out the importance of such studies (Uenishi, 2010, Chen & Li., 2015). In a congested urban environment such as a transportation hub, large underground chambers and building clusters coexist. Underground chambers have been hinted to modify ground motions (Dashti et al., 2016), yet, comprehensive studies on wave propagation and soil response are further needed to better understand the soil-structure-underground structure interaction (SUSSI) phenomenon. The aim of this paper is to explore the importance and impact of underground structures in a congested transportation-hub on surface ground motions, along with SCI effects. Findings presented herein further highlight that fully integrated 3D analyses considering realistic settings of above and underground-structures are important for resilient seismic design of urban cities.

2. THREE DIMENSIONAL COMPUTATIONAL PLATFORM

The greatest challenges in numerical modelling of site-city interaction lie in the effectiveness of the numerical method and the computational platform for solving 3D elastic wave propagation and meshing complex 3D geometries. The spectral element method is widely accepted by the research community and regarded as one of the most effective numerical approaches for dealing with wave propagation problems (Komatitsch & Vilotte, 1998, Faccioli, et al., 1997). Meshing becomes a major issue for multi-scale simulations, i.e. small detailed geometries in a large domain (e.g. urban site upon soil medium), especially when using a spectral element method, which requires hexahedral meshes. Unstructured non-conforming (i.e. discontinuous) meshes can easily overcome such a challenge. In terms of efficiency, the key concern is parallel capabilities of the numerical code. All aforementioned qualities are present in the numerical platform SPEED (Mazzieri, et al., 2013), which makes it an excellent tool for the investigation of SCI effects.
SPEED uses the discontinuous Galerkin discretization coupled with the spectral element (DGSE) method to solve a weak formulation of the elastodynamic wave equation. The DGSE method can solve wave propagation on non-conforming unstructured hex meshes with sharp changes in size and polynomial degree (h and N adaptivity). It utilizes jump and penalty functions at discontinuous interfaces to ensure compatibility, thus retaining satisfying accuracy and high flexibility for meshing. Numerical discretization of the governing equations uses Lagrange-polynomial basis functions of N degree and the Lagrange-Gauss-Lobatto integration rule on quadrature points coinciding with spectral nodes, resulting in a diagonal mass matrix to guarantee numerical efficiency. The time marching scheme used is the standard leapfrog, which requires the satisfaction of the CFL condition and a minimum number of 5 spectral nodes per wave length to limit grid dispersion and dissipation.

3. MODELING OF BUILDINGS AND UNDERGROUND STRUCTURES

The chosen site, Kowloon metro station, is one of the busiest transportation hubs in Hong Kong surrounded by super-tall buildings, including the International Commerce Centre the tallest skyscraper of Hong Kong. The arrangement of the structures, as shown in Fig.3.1, is typical for such hubs in Hong Kong. Kowloon station is a priority site as it is subjected to further development, vastly populated and represents high economic value.

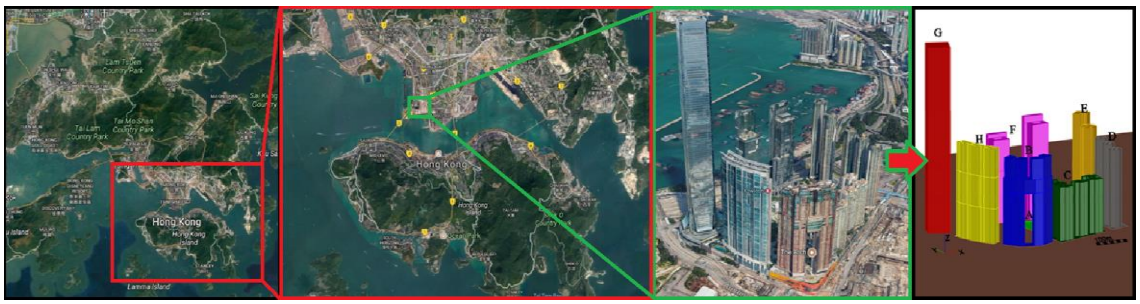

Figure 3.1 Study site – Kowloon metro station, Hong Kong

3.1. Computational models

In order to examine SUSSI and SCI effects, two models are created. One is comprised of the high-rise building cluster alone, hereafter referred to as ‘structure model’, and the other includes both the building cluster and the metro station, referred to as ‘metro model’ in the following, see Fig.3.2. Geometric and geological properties of the models are based on architectural, geotechnical and geological data acquired from the Hong Kong Buildings Department. The simulation domain is 1.8×1.8×0.12 km in size, while the area of the urban development is 1.4 km^2. The urban density, i.e. the areal ratio between the total develpment surface and the surface covered by buildings, is θ_s=0.0154 and θ_m=0.02 for the site without and with the metro station respectively.There are seven building clusters and the metro station (A-H) at the site as shown in Fig.3.2. and described in Table 4.2. The variation in both height and complexity of the structural systems is large resulting in significant inertial differences between the two sides of the hub, specifically the areas around structures G, H, B and C-F.
A regular 20×20m grid of monitoring points on the top of the soil domain is utilized to track surface displacements. Data derived from the recordings on the grid are subsequently animated and highlighted in cartoons.

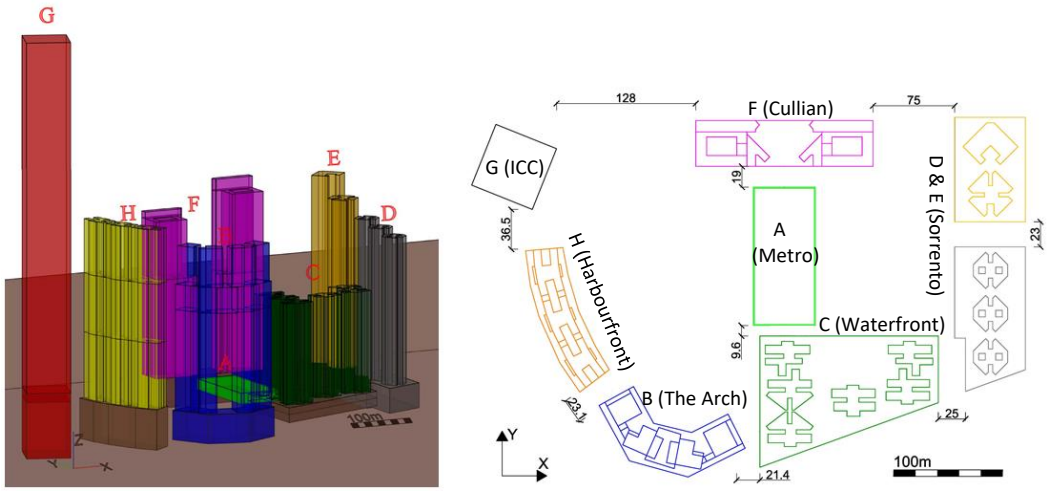

Fig.3.2 3D X-Ray plot and layout plan of the metro model

3.2. Meshing

Owing to the capabilities of SPEED to deal with non-conforming meshes, the meshing procedure is straightforward. AutoCAD was used to create and decompose the geometry into meshable volumes. Consequently, the geometry was imported to the meshing software TRELIS, which enables the utilization of advanced meshing techniques to generate the desired unstructured non-conforming mesh in high quality. Figure 3.3 shows the meshed geometry and the scaled Jacobians for the generated mesh. The model consists of 452,400 elements in total, of which solely 0.1% are below good quality. Note that a hex element is regarded as good quality if its scaled Jacobian is above 0.5, while elements below 0 or 0.2, depending on the simulation software, are unacceptable for numerical analyses.

An average mesh size of 5m and 10m were set for the structures and the soil domain, respectively. Discontinuous interfaces are employed between soil and structure meshes to ease an otherwise gruelling task of meshing the complex geometry of the urban development. In Fig.3.3, interfaces between different coloured blocks are non-conforming.

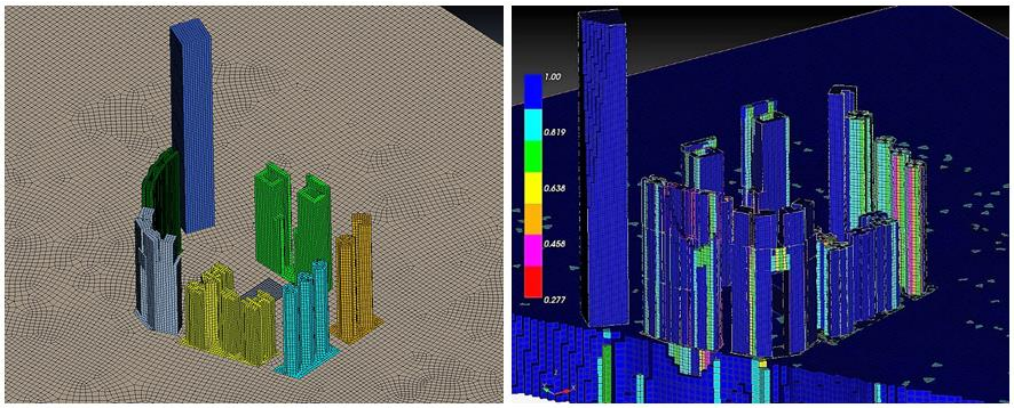

Figure 3.3. The meshed geometry and its scaled Jacobian values as an indicator of quality

4. SIMULATION AND MODEL PARAMETERS

4.1. Soil domain

The soil domain is a 1.8×1.8×0.12 km viscoelastic layer-cake model comprising of three different materials, described in Table 4.1, subjected to an ‘x’ polarized plane wave. Displacements in ‘y’ and ‘z’ directions are restricted on the sides of the domain, while an absorbing boundary condition is prescribed at the bottom surface to ensure halfspace conditions. The natural frequency of the site is f_s=1Hz, hence an SH wave in the form of a 1Hz displacement Ricker wavelet is used as the input motion for the sake of site resonance. Since the spectral

acceleration for the 2475-year return period uniform hazard spectrum on the rock outcrop is 0.93 m/s^2 at 1Hz for Hong Kong (ARUP, 2015), the amplitude of the wavelet is first determined by fitting this spectral value. Then, the rock outcrop motion is deconvoluted to a within motion which gives an excitation with 0.945 mm peak displacement. SPEED adopts damping through a frequency proportional quality factor (Q), here Q=10 (ζ=5%) and Q=25 (ζ=2%) evaluated at 3Hz are adopted for soil and rock, respectively. Stiffness increase of the completely decomposed granite (CDG) layer due to overburden pressure is accounted for by increasing V_s at each layer. Borehole and SPT N data are utilized to determine geological properties of each soil layer (Wair et al., 2012). Note that V_p=2V_s is adopted for compression wave velocity.

Table 4.1 Soil layer properties

Id.	Soil type	Layer thickness [m]	SPT N	V_s [m/s]	ρ [g/cm^3]	h [m]	N
1	Fine sand fill	30	28	230	1.95	10	3
2	CDG	30	50	400	1.95	10	3
3	CDG	20	70	450	1.95	10	3
4	CDG	20	80	480	1.90	10	3
5	Granite	30	>200	2000	2.60	10	3

4.2 Foundation-superstructure system and metro station

The foundation-superstructure system is modelled as viscoelastic equivalent blocks consisting of the same hexahedral elements as the soil. The blocks are homogeneous and their parameters are determined in accordance with the dynamic parameters of each structure. The shear wave velocity and natural period of each structure, listed in Table 4.2, are roughly estimated using Eq. 4.1 and Eq. 4.2.

$$V_s = 28h_s \tag{4.1}$$

$$T_s = \frac{N_s}{10} \tag{4.2}$$

where h_s is the inter-story height, T_s is the natural period of the building and N_s is the number of stories.
The natural frequency of the buildings is in the range of 0.09-0.2 s, and most of them are around f_b=0.14Hz, which defines a frequency ratio between the soil and the structures of f_s/f_b=7.14. Mass density and quality factor for each equivalent block is set to ρ=300kg/m^3 and Q=10 (ζ=5%) (Taborda & Bielak., 2011). Polynomial degrees of the interpolation function were set to N=3 and N=2 for the superstructures and foundations, respectively to ensure optimal numerical resolution and flexural behaviour.
The natural periods of foundations, T_f, were estimated using Eq. 4.3. Their shear wave velocity (V_s) and mass density (ρ) were determined by averaging the stiffness (note G= ρV_s^2) and density of the soils and concrete weighted by their areal ratio, see Eq. 4.4 and Eq. 4.5.

$$T_f = \frac{4h}{V_s} \tag{4.3}$$

$$V_s^f = \frac{A_p}{A_f}\sqrt{\frac{G_c}{\rho_c}} + (1-\frac{A_p}{A_f})\sqrt{\frac{G_s^{avg}}{\rho_s^{avg}}} \tag{4.4}$$

$$\rho_f = \frac{A_p}{A_f}\rho_c + (1-\frac{A_p}{A_f})\rho_s^{avg} \tag{4.5}$$

where h is the depth of each foundation, A_p is the total cross-section area of piles, A_f is the total foundation area, G_s^{avg} and ρ_s^{avg} are the averaged stiffness and density of soils encompassing the piles, ρ_c and G_c are density and stiffness of concrete, respectively.
The metro station is modelled by a closed rigid box. The box has 1m thick walls, dimensions 57×127×15m and its top is on the level of the ground surface. A polynomial degree of N=1 is used for the basis function as the flexural deformation of the walls are expected to be low due to high rigidity, moreover the box is assumed to move together with the ground. The primary goal is to capture SUSSI, i.e. how the metro station modifies ground motions due to its hollow nature and imposing impedance difference. The properties of all structure models, including identification, are listed in Table 4.2 and visualized in Fig.3.2.

Table 4.2 Structure properties and identifications

Id	Name	Structure	Story height/ Soil-pile ratio	Height/ Depth [m]	Natural frequency [Hz]	V_s [m/s^2]	ρ [g/cm^3]	G_{avg} [Mpa]
A	Metro	Super structure	15	15	-	1250	2.5	3906.3
		Foundation	-	-	-	-	-	-
B	The Arch	Super structure	3.2	225	0.14	90	0.3	2.4
		Foundation	0.1042	40	4.27	683	2.01	937.0
C	Waterfront	Super structure	2.8	138	0.20	78	0.3	1.8
		Foundation	0.0366	20	5.49	439	1.97	379.6
D	Sorrento short towers	Super structure	2.95	208	0.14	83	0.3	2.0
		Foundation	0.065	34	4.10	557	1.99	617.1
E	Sorrento tall towers	Super structure	3.15	243	0.13	88	0.3	2.3
		Foundation	0.065	34	4.10	557	1.99	617.1
F	The Cullian	Super structure	3.3	242	0.14	92	0.3	2.6
		Foundation	0.1042	40	4.27	683	2.01	937.0
G	ICC	Super structure	4.3	480	0.09	120	0.3	4.3
		Foundation	0.2333	89	2.75	980	2.08	1996.4
H	Harbourfront	Super structure	3	245	0.12	84	0.3	2.1
		Foundation	0.1661	55	3.81	839	2.04	1436.9

5. RESULTS

Displacement history is gathered at each monitoring grid point from which accelerations (a), and two special descriptors, namely ground perturbations (d_p) and velocity signal energy (E), are derived. Perturbations, as expressed in Eq.5.1, represent the relative displacement between two sets of displacement time histories. It aims to highlight radiated wavefields and ground motion disturbance at the examined nodes via,

$$d_p(t) = d_2(t) - d_1(t) \tag{5.1}$$

where $d_p(t)$ is the perturbation time history, $d_1(t)$ and $d_2(t)$ are the displacement histories to be compared, (e.g. the freefield and displacements of the structure model). The velocity signal energy, defined in Eq.5.2, is descriptive of the kinetic energy of the ground that highlights the power contained in the reaction of the soil and its potential to generate large inertial effects (Bard, et al., 2006):

$$E = \int_{t0}^{T} v(x,t)^2 dt \tag{5.2}$$

where $v(x,t)$ is the ground velocity at x, integrated through the signal duration.
The recorded data and principal findings are detailed in the followings through the aforementioned parameters. The results show that SPEED is capable of capturing the complex interaction of SCI and SUSSI. Deamplification and decreased spatial coherency of ground motions well described in previous studies (Semblat, et al., 2008, Taborda & Bielak., 2011, Lombaert, et al., 2004) are apparent from the results. Two key parameters in SCI highlighted by Bard et al. (2006) and Guéguen et al. (2002), namely the urban density and the frequency ratio, see section 3.1 and 4.2, would indicate SCI is not favoured for the present case, however noteworthy changes in signal energy are observed in a well-defined pattern.
Acceleration snapshots are shown in Fig. 5.1 for two different time-steps. Accelerations show significant incoherencies within the urban area. Inertial effects are very strong on the left side (F, G, B) due to a much larger mass concentration and deeper foundation depths, while in the middle of the building layout, accelerations are focused and amplified compared to freefield motions. SSSI effects are clearly present. At the hub outskirt (t=1.3s) and outside the development area (t=1.7s), circular zones of higher acceleration are a clear sign of building vibration feedback to the soil (SSSI). The distinctive circular radiation and focus of ground motions, outside and amid buildings, respectively, indicate a great significance of the building layout, even though these structures have vastly different fundamental frequencies and shapes. The radiated acceleration field travels up to 500m with a maximum amplitude of 0.3m/s^2, in excess to freefield motions. This imposes additional demand on buildings around the urban area equivalent to 50% of a serviceability level earthquake (SLE) (Chinese Standard.,

2008). The presence of the metro station favourably modifies the ground motions and spatially divides the focused zone in the centre.

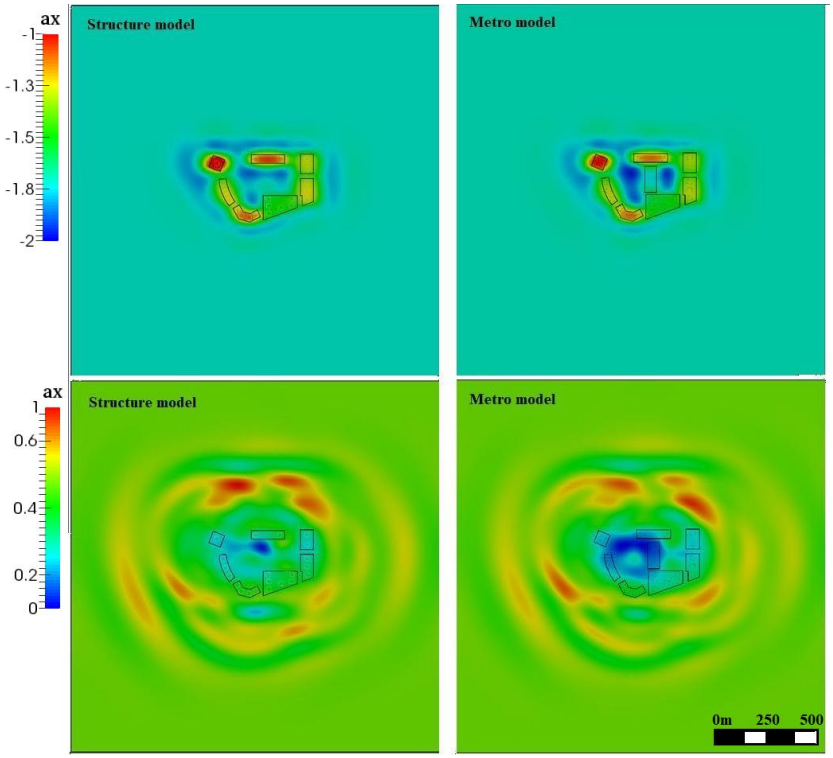

Figure 5.1 Acceleration at 1.3 s (max acceleration inside the cluster) and at 1.7s (radiated wavefield)

Signal energy ratios are presented for the models compared to freefield energy and to each other in Fig.5.2. Kinetic energy of the soil for the structure model is up to 135% and 110% of the freefield energy, while for the metro model it is 120% and 110% in the centre of the development area and the outskirt, respectively. This highlights the deamplification phenomenon produced by the metro station. The expanse of the effect is limited to the close vicinity of the station, as shown by the bottom cartoon in Fig.5.2. The station box divides the focused amplification zone at the urban centre into two smaller zones. Results suggest that the smaller the unbuilt zone between buildings, the smaller the kinetic energy of the soil, though no definite conclusions can be drawn at this point. However, it is worthy to highlight the fact that the zone of focused energy mimics the geometry of the unbuilt zone, furthermore it is skewed towards lighter buildings with shallower foundations (C) This suggests a strong pinning effect of the foundations and a 3D SUSSI wave-trapping phenomenon by subsurface structures. The pinning effect in conjunction with a strong inertial effect is pronounced for heavier buildings with deeper and stiffer foundations (F, G, H, and B). A 20% reduction in ground kinetic energy is observed in the vicinity of the structures, resulting from SSSI and overall stiffening of the site response, due to change in overall mass. However, building shape and orientation also shows a strong influence on reducing ground kinetic energy. This is apparent by examining energy ratios around buildings F and H. Both structures are of similar weight and foundation depth, however structure H is oriented unfavourably, i.e. it has a lower flexural stiffness in the direction of excitation, while structure F is oriented in the most favourable manner. Despite unfavourable key SCI indicators, such as a high f_s/f_b ratio, significant SCI effects can arise due to strong inertial effects as hinted by Kham et al. (2006). However, a clear radiation pattern is observed in this study in spite of large mass differences between buildings, which is suggested to cause the chaotic irregularity of ground motions by Kham et al. (2006). The key features are shown to be the distance between buildings and their reaction or activation to ground shaking rather than the weight difference between them. Structural reactions can be traced back to their stiffness, vibration modes and orientation with respect to shaking direction (e.g. F vs. H). The signal energy and ground motions in the ring around structures are largely homogeneous. The energy field is only disturbed between G and F due to their larger distance (see Fig.3.2.), in direct vicinity of structures (few meters), and in the unbuilt zone within the building layout, see Fig 5.2 and Fig 5.3. Furthermore, it is recommendable to revisit the concept of urban density as an indicator for SCI effects. For special urban layouts, e.g. large squares encompassed by tall buildings, more specific description of the urban density should be considered by factors such as the number of buildings, distance between neighbours and the open area embraced by structures, rather than a homogenized indicator such that the surface ratio θ.

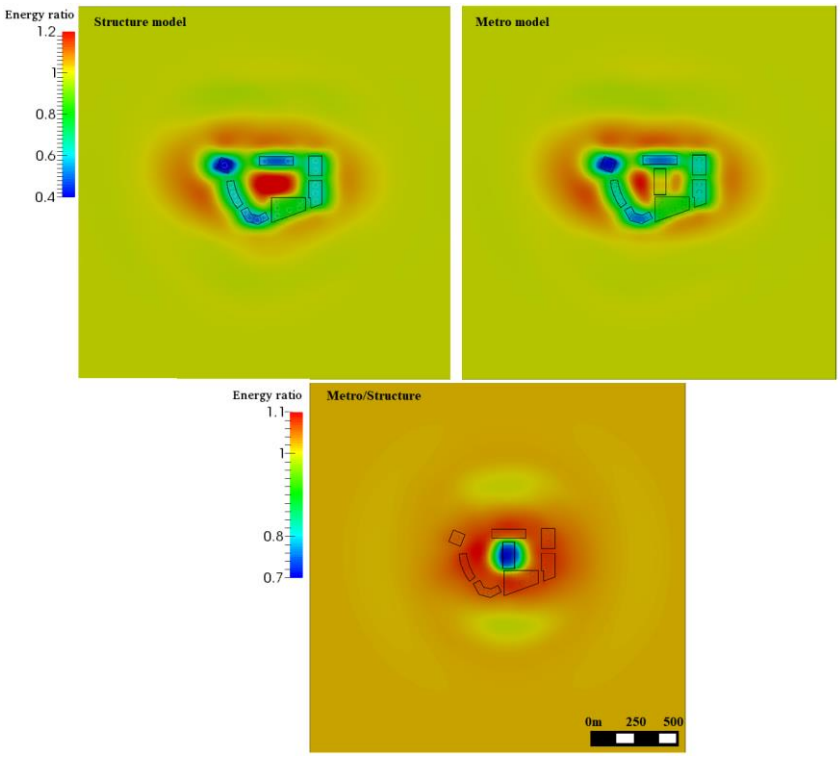

Figure 5.2 Signal energy ratios between each model and the freefield (top) and between the two models (bottom)

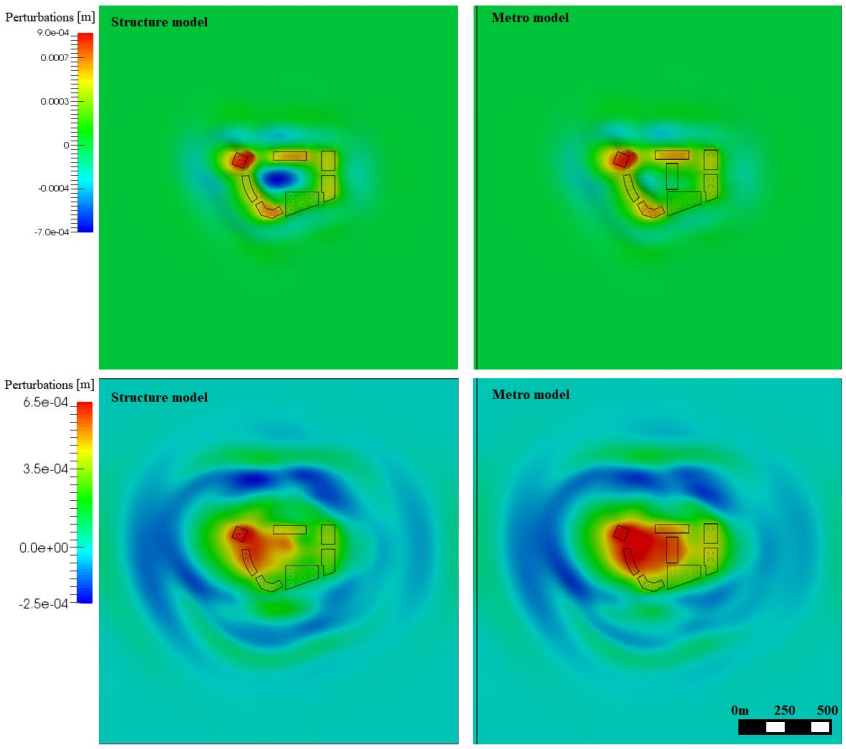

Figure 5.3 Perturbations at 1.7s (max d_p) and at 2.7s (radiated wavefield)

Ground motion perturbations are highlighted in Fig.5.3. Similar phenomena can be identified through the perturbation wavefield. The top pair of cartoons highlight the impact of the metro station on ground displacements. Perturbations are reduced and smoothed out due to underground opening of the metro station. It ties the soil around its area into the movement of the building cluster and results in a more homogeneous movement of the urban development. The bottom right cartoon further illustrates this response. It is worth to

note that the smaller the unbuilt zone between structures the smaller the focused zone of amplification. This is apparent by examining the perturbations on the right and on the left to the metro station in the metro model. In the larger unbuilt zone (left) perturbations persist, conversely in the smaller zone (right) perturbations are faintly present. Hence, underground structures closely spaced to other structures representing significant weight favour SCI, therefore they should be accounted for, when evaluating urban density. The bottom pair of cartoons in Fig.5.3 on the bottom highlights the strong inertial effect of the zone carrying heavy structures (G, H) with unfavourable orientations, such that perturbations are stronger on the left side of the transportation hub. It further displays the feedback vibrations generated and radiated outwards by the urban site in a distinct circular pattern. Perturbations within both the transportation hub and the radiated wavefield reach up to 25% of the maximum freefield displacements, which reemphasizes the concern for structures built in the outskirt of congested urban sites.

6. CONCLUSIONS

The aim of this study was to explore SUSSI and SCI effects by means of realistic, fully integrated 3D simulations of a transportation hub. Velocity signal energies and perturbations reveal significant SCI interactions, despite large differences in the natural frequencies between buildings and site. This can be correlated to three factors: strong inertial effects stemming from the mass of super-tall buildings, pinning effects of deep foundations and the proximity of structures. Consistent patterns in soil energy and the propagated wavefield are governed by the layout of buildings and subsurface structures, highlighting the importance of considering realistic geometries. The commonly appearing metropolitan square or circular layout of buildings, such as the test site of this study may be subjected to increased seismic demand during earthquakes. Focused zones of amplification emerge at the unbuilt areas in the centre plaza and the outskirt of these development areas. The presence of the metro station, with large underground opening, serves to reduce the zone of amplification in the centre plaza in this analysis. The metro station has an important role in SUSSI through trapping of waves between structure foundations and itself. The perturbed wavefield at unbuilt zones amid structures are more homogenized, thus the adverse effect of SCI is reduced.

AKCNOWLEDGEMENT

The authors acknowledge support from Hong Kong RGC grant no. 16213615 and Intergroup Collaborative Research Program from the Department of Civil and Environmental Engineering of HKUST.

REFERENCES

1. ARUP (2015). Seismic Hazard Analysis of the Hong Kong Region. GEO Report No. 311.
2. Bard, P., Chazelas, J., Guéguen, P., et al. (2006). Site-City Interaction. In: C.S. Oliveira, A. Roca and X. Goula (eds.), Assessing and Managing Earthquake Risk, Springer, 91-114.
3. Çelebi, M., Bazzurro, P., Chiaraluce, L., et al. (2010). Recorded motions of the 6 April 2009 Mw 6.3 L'Aquila, Italy, earthquake and implications for building structural damage: overview. *Earthquake Spectra*. **26: 3,** 651-684.
4. Chen, Q. & Li, W. (2015). Effects of a group of high-rise structures on ground motions under seismic excitation. *Shock and Vibration.* **2015:**
5. Chinese Standard (2008). G 50011-2010, "Code for Seismic Design of Buildings".
6. Dashti, S., Hashash, Y., Gillis, K., et al. (2016). Development of dynamic centrifuge models of underground structures near tall buildings. **86:** 89-105.
7. Faccioli, E., Maggio, F., Paolucci, R. and Quarteroni, A. (1997). 2D and 3D elastic wave propagation by a pseudo-spectral domain decomposition method. *Journal of Seismology.* **1: 3,** 237-251.
8. Flores, J., Novaro, O. and Seligman, T. (1987). Possible resonance effect in the distribution of earthquake damage in Mexico City. *Nature*. **326: 6115,** 783-785.
9. Gueguen, P. & Bard, P. (2005). Soil-structure and soil-structure-soil interaction: experimental evidence at the Volvi test site. *Journal of Earthquake Engineering*. **9: 05,** 657-693.
10. Guéguen, P., Bard, P. and Chávez-García, F. J. (2002). Site-city seismic interaction in Mexico city–like environments: an analytical study. *Bulletin of the Seismological Society of America.* **92: 2,** 794-811.
11. Jennings, P. C. (1970). Distant motions from a building vibration test. *Bulletin of the Seismological Society of America.* **60: 6,** 2037-2043.
12. Kham, M., Semblat, J., Bard, P. and Dangla, P. (2006). Seismic site–city interaction: main governing

phenomena through simplified numerical models. *Bulletin of the Seismological Society of America.* **96: 5,** 1934-1951.
13. Komatitsch, D. & Vilotte, J. (1998). The spectral element method: An efficient tool to simulate the seismic response of 2D and 3D geological structures. *Soil Dynamics and Earthquake Engineering.* **88: 2,** 368-392.
14. Lombaert, G., Clouteau, D., Ishizawa, O. and Mezher, N. (2004). The city-site effect: a fuzzy substructure approach and numerical simulations. The 11th International Conference on Soil Dynamics and Earthquake Engineering and 3rd International Conference on Earthquake Geotechnical Engineering.
15. Mazzieri, I., Stupazzini, M., Guidotti, R. and Smerzini, C. (2013). SPEED: Spectral Elements in Elastodynamics with Discontinuous Galerkin: a non-conforming approach for 3D multi-scale problems. *International Journal of Numerical Method in Engineering.* **95: 12,** 991-1010.
16. Semblat, J., Kham, M. and Bard, P. (2008). Seismic-wave propagation in alluvial basins and influence of site-city interaction. *Bulletin of the Seismological Society of America.* **98: 6,** 2665-2678.
17. Schwan, L., Boutin, C., Padrón, L., et al. (2016). Site-city interaction: theoretical, numerical and experimental crossed-analysis. *Geophysical Journal International.* **205: 2,** 1006-1031.
18. Taborda, R. & Bielak, J. (2011). Full 3D integration of site-city effects in regional scale earthquake simulations. Oral Presentation at 8th International Conference on Structural Dynamics.
19. Uenishi, K. (2010). The town effect: dynamic interaction between a group of structures and waves in the ground. *Rock Mechanics and Rock Engineering.* **43: 6,** 811-819.
20. Wair, B. R., DeJong, J. T. and Shantz, T. (2012). Guidelines for estimation of shear wave velocity profiles. Technical Report 2012/08, Pacific Earthquake Engineering Research Center.